Cellular and Molecular Biology

Dodel *et al. Cell. Mol. Biol.*2016, 62 (10): 16-25
ISSN: 1165-158X
doi: 10.14715/cmb/2016.62.10.3

Original Research

Modifying the mechanical properties of silk nanofiber scaffold by knitted orientation for regenerative medicine applications

M. Dodel[1], N. Hemmati Nejad[1*], S. H. Bahrami[1], M. Soleimani[2*], H. Hanaee-Ahvaz[3]

[1] Textile Engineering Department, Amirkabir University of Technology, Tehran, Iran
[2] Hematology Department, Faculty of Medical Science, Tarbiat Modares University, Tehran, Iran
[3] Stem Cell Technology Research Center, Tehran, Iran

Abstract: Tissue reconstruction is among the increasing applications of polymer nanofibers. Fibrous scaffolds (mats) can be easily produced using the electrospinning method with structure and biomechanical properties similar to those of a cellular matrix. Electrospinning is widely used in the production of nanofibers and the GAP-method electrospinning is one of the means of producing fully aligned nanofibers. In this research, using the GAP-method, knitted fibrous scaffolds were made of silk fibroin, which is a biocompatible and biodegradable polymer. To extract fibroin from cocoons, the sodium chloride solution as well as dialysis and freeze-drying techniques were employed. The molecular weight of the extracted fibroin was measured with the SDS-Page electrophoresis technique. Moreover, the pure fibroin structure was examined using the ATR-FTIR method, and the viscosity of the solution used for electrospinning was measured with the Brookfield rotational viscometer. The scaffolds were prepared through electrospinning of the silk fibroin in pure formic acid solution. The following three structures were electrospun: 1) a random structure; 2) a knitted structure with an interstitial angle of 60 degrees; 3) a knitted structure with an interstitial angle of 90 degrees. Morphology of the resulting fibers was studied with a SEM (scanning electron microscope). Fibroin scaffolds are degradable in water. Therefore, they were fixated through immersion in methanol to be prepared for assays. The mechanical properties of the scaffolds were also studied using a tensile strength test device. The effect of methanol on the strength properties of the samples was also assessed. The hydrophilic potential of the samples was measured via a contact angle test. To increase the hydrophilicity of the scaffold surfaces, the cold oxygen plasma technique was employed. Finally, the biocompatibility and cell adhesion of the resulting scaffolds were examined through a HEK 293 cell culture, and the results were analyzed through the MTT, DAPI staining, and SEM imaging techniques. Results revealed that the oriented knitted structure contributed to the increase in Young's modulus and the maximum strength of scaffolds as compared to the random samples. Moreover, this structure can also be a suitable alternative to the typical chemical means of increasing strength.

Key words: Silk fibroin, electrospinning, nanofiber, knitted scaffold, mechanical properties, regenerative medicine.

Introduction

The silk obtained from B. mori worms has been used for the commercial production of suture. Hence, the effectiveness of silk as a suitable biomaterial has been proven. Natural silk contains two major protein structures: 1) Fibroin (which forms the largest part of natural silk); and 2) Sericin (which is a water-soluble resinous protein surrounding fibroin fibers and binding them together coherently). Research indicated that fibroin has considerable properties such as satisfactory strength, satisfactory biocompatibility, optimal oxygen and moisture permeability. This material can also be produced in different forms such as fiber, film (membrane), gel, and sponge. Extensive research is currently being conducted in the world on the applications of silk fibroin to three-dimensional structures in different fields including tissue engineering, regenerative medicine, drug release, and the like. Numerous technologies have been used to design materials to properly simulate the ECM structure. Some of these technologies include electrospinning, self-assembly, phase separation, etc. The production of nanofiber scaffolds through electrospinning is among the most popular three-dimensional structure synthesis methods after silk fibroin. These scaffolds have been used in numerous studies in the past decade. In the field of tissue engineering, electrospinning is commonly used as a simple method for producing non-woven scaffolds with submicron structures (1-4). Although there has been concern for the applications of silk fibroin in tissue engineering for the production of polymer nanofibers as well as bone, cartilage, and muscle tissues, the strength of silk fibroin is slightly lower than the optimal strength for ligament and tendon tissue engineering (5,6). Many researchers have focused on optimization of the diameter of nanofibers produced by electrospinning, and there has been little concern for the alignment of the final scaffolds (7, 8). Similarly, extensive efforts have been made to increase the strength of this material based on its production form and the post-production chemical operations. In the various tested methods, the physical structure and texture of the resulting scaffolds were slightly considered (9-11). Gholipourmalekabadi et al. showed that formic acid is a suitable solvent for the production of nanofibers with appropriate fiber diameter distributions and good biocompatibility. Formic acid increases the crystallinity of silk fibroin by reinforcing the inter-chain hydrogen bonds of silk fibroins

Received February 29, 2016; **Accepted** August 2, 2016; **Published** August 31, 2016

*** Corresponding author:** Nahid Hemmati Nejad, Textile Engineering Department, Amirkabir University of Technology, Tehran, Iran. Email: hemmati@aut.ac.ir or Masoud Soleimani**,** Tarbiat Modares University, Jalal Ale Ahmad Highway, 14115-111, Tehran, Iran. Email: soleim_m@modares.ac.ir

and producing more β-sheet structures. As a result of this process, the hydrodynamic radius of fibroin is minimized (1, 12-13). On the other hand, this solvent produces thinner fibers than the typical HFIP solvent, because it has a higher vaporization speed than HFIP and provides fibers with enough time to extend (1). In the present study, using the pure formic acid solvent, an attempt was made to produce nanofiber scaffolds from silk fibroin through the unique and special Gap Electrospinning method. This method is easy to use and creates a knitted structure with the desired interstitial angles. As a result of this alignment and engineered structure, the strength of the final scaffold is modified with satisfactory precision. Assessments in this research aimed to reveal the positive effect of knitted alignment of silk fibroin nanofibers on the ultimate strength of this structure as compared to random structures. In addition, it was indicated that the alignment has no adverse effect on the interaction between the cell and scaffold surface, while porosity and degradability of the scaffold is also improved.

Materials and Methods

Fibroin extraction from silk cocoons

B. Mori silk cocoons were purchased from the Gilan Silk Production Factory, Iran. The worms were removed from the cocoons, the cocoons were cut into segments using a special clamp, and different fiber surfaces were separated. The fibers were put in a 0.02 molar Na_2CO_3 aqueous solution and were boiled for 30 minutes. Afterwards, the fibers were removed from the solution and were washed with water for 20 minutes. The washing was repeated three times. The excessive water of fibers was collected (dried) and the fibers were stored at room temperature to become dried (2, 3, 14-16). Next, a solution with molar ratio of 8:2:1 for $CaCl_2$: Ethanol: Water was prepared and a specific amount of degummed dried fibers was added to the solution. The mixture was stored at a temperature of 60 degrees for 4 days and was mixed gently. Next, the solution was poured into a dialysis bag (cut-off=14 KDa) and was dialyzed for 48 hours in ultra-pure water. The solution was then transferred from the dialysis bag to a falcon and was centrifuged twice at a moderate rpm. The upper solution containing fibroin was dried through the freeze-dry method and the resulting pure fibroin was used to continue the experiments and carry out the required analyses (15-18).

Molecular mass determination by SDS-page electrophoresis

The molecular weight of the resulting fibroin was measured through SDS-Page electrophoresis (14, 17). In vertical one-dimensional electrophoresis, as proteins pass through the polyacrylamide gel matrix to reach the anode (+), they are separated based on their molecular size. To this end, 1cc of a solution containing 100 ng of pure fibroin was prepared using distilled water. The 10-150 KDa standard was used for this purpose and the device in use was a product of the American BioRAD Company.

ATR-FTIR analysis

The structure of silk fibroin in the final scaffolds was examined via ATR-Fourier transform infrared (ATR-FTIR) spectroscopy. The spectroscope was manufactured by Bruker Company in Germany. The device was equipped with a DTGS detector and ATR diamond crystal. For testing purposes, 1 mg of the sample and 300 mg of KBr were used to make a tablet under vacuum conditions, and examinations were carried out from 600 cm^{-1} to 4000 cm^{-1} with a resolution of 4 cm^{-1}. Results of this analysis were used to show the presence of special chemical groups of silk fibroin (3, 15, 19).

Viscosity measurement

Prior to electrospinning, the viscosity of the resulting solution was measured using a rotational viscometer. For this purpose, a 20% wt. fibroin in pure formic acid (Merck) solution was used. The viscometer was employed at a temperature of 30 degrees and at various velocities in the 100 to 150 rpm range (3, 6). The viscometer was a DV III model manufactured by Brookfield Company in the United States.

Electrospinning procedures

Electrospinning was used to produce random and knitted nanofiber scaffolds with interstitial angles of 60 and 90 degrees. The electrospinning conditions were the same for all of the three scaffold types. However, a circular cylindrical drum with low rpm was used for random scaffolds and a GAP-based collector drum was used for knitted scaffolds (20). A 15 Kv voltage, a nozzle-collector spacing of 10 cm, and an injection rate of 0.3 ml/h were used to produce uniform fibers without beads and with diameters of several nanometers. The electrospinning solution was prepared with 20% wt. in pure formic acid. The electrospinning device was a Nanospinner made by Stem cell Technology Company in Iran (21-28).

Mechanical properties

The tensile properties of scaffolds were measured in fixed and non-fixed states using a Universal Testing Machine manufactured by the SANTAM Company in Iran. The samples were prepared in 10x50 mm^2 dimensions with a thickness of 40 micrometers. The shearing procedure for knitted samples was carried out such that the tension axis was perpendicular to the interstitial angle. The stress-strain graphs of samples were obtained and reported using the device software. Measurements were repeated three times for each sample (21,23,29).

Degradation behavior

The scaffolds degradability rates resulted from immersion of samples in PBS (37°C and pH=7.5) were calculated for different periods. At the end of each period, the samples were washed and dried up at ambient temperature in an oven (3, 22). The degradation rate was calculated as follows:

$$D_t = (W_0 - W_t)/W_0 \times 100 \quad (1),$$

Where,

W_0 = Initial weight of each sample.

W_t = Weight of samples following immersion and drying.

Methanol soaking cross-linking method

To reduce the degradation rate of scaffolds and

increase their strength, the samples were immersed in pure methanol (Merck). The electrospun scaffolds were submerged in pure methanol for 30 minutes after 24 hours of storage in a vacuum oven at room temperature. Afterwards, the scaffolds were moved out of the oven and were stored for 24 hours at ambient temperature to dry up. Next, the scaffolds were kept for 24 hours in a vacuum oven at a temperature of 30 degrees to fully remove the remaining methanol from the scaffolds (3, 30).

Hydrophilicity evaluation of fixed scaffolds

Fixation of fibroin scaffolds with methanol led to a reduction in their surface hydrophilicity. Moreover, hydrophilicity of scaffold surfaces was examined by measuring the contact angles. The contact angles with water were measured on the surface of scaffolds before and after the surface plasma treatment. The experiment was carried out using a G10 Kruss made in Germany and the sessile drop technique (29).

Surface plasma treatment

To increase the hydrophilic property of the surface of fibroin scaffolds fixed with methanol, low-pressure oxygen plasma was applied to the scaffold surfaces. To this end, the Nano-plasma device made by Diener Company in Germany was employed. The procedure was carried out at a frequency of 40 KHz using pure oxygen (as the gas) with a power of 30 watts and duration of 5 minutes (23, 24-27).

Cell seeding

Plasma-treated scaffolds were punched in the form of circles with a diameter of 1 cm, and the circles were put in 24-well TCPS (tissue culture polystyrene) cell culture plates. The scaffolds were sterilized through 3 hours of submersion in 70% ethanol under a sterile hood. Next, the scaffolds were immersed in DMEM (Dulbecco's Modified Eagle Medium) and were incubated for 24 hours to ensure their sterility. Afterwards, 100 microliters of DMEM containing 10% of FBS (fetal bovine serum) and $30x10^3$ HEK 293 cells (Human Embryonic Kidney 293) were added gradually to each scaffold in a step-wise process. After 30 minutes, 800 microliters of DMEM containing 10% of FBS (fetal bovine serum) was added to each scaffold and the scaffolds were incubated (22, 29).

Structural morphology

Scanning electron microscopy (SEM)

Morphology of scaffold surfaces was assessed before and after cell culture using a LEO1455VP SEM (scanning electron microscope) made in England. Samples were coated with a thin conductive layer of gold in vacuum conditions prior to analysis. The diameter of fibers was also measured in Image Analysis (Image J, US) based on the resulting SEM images (26, 28, 29).

Porosity

Porosity of each sample was calculated via the following formula:

$$\text{Porosity} = (1 - \rho/\rho_0) \times 100 \quad (2),$$

Where p is density of the electrospun scaffold and p_0 is the polymer density (31).

In-vitro biocompatibility evaluation

MTT assay

A comparison was drawn using the MTT analysis method between the cell proliferations on electrospun scaffolds and TCPS cell culture plates. The sterilized scaffold punches were put inside a 24-well plate. For each well with a density of $30x10^3$, the HEK 293 cell line was cultured on the scaffolds, and the scaffolds were put in an incubator at a temperature of 37°C and CO_2 level of approximately 5%. On the first, third, fifth and seventh days of cell culture, 500 microliters of MTT solution (5 mg/ml) was added to each well and the samples were put in the incubator at a temperature of 37°C for two hours. To solve dark-blue intracellular formazan, first the upper liquid was removed and then 200 microliters of DMSO was added to the wells. In scaffold-containing wells, first the scaffold was moved out of the medium containing the MTT solution, and then DMSO was added via a micro tube to omit the effect of cells separated from the scaffold surface. The process was repeated three times for each sample. The optical density of samples was measured with a spectrophotometer at the 570 nm wavelength (25, 26, 28, 29).

Cell adhesion evaluation by SEM

To check a single-cell adhesion to the scaffold surfaces, a total of $20x10^3$ HEK293 cells (Human Embryonic Kidney 293 line) were cultured on a circular scaffold with a diameter of 1cm, and the scaffold was prepared and transferred on the third day for SEM imaging. First, the scaffold and cells were washed with PBS and were fixed in 2.5% Glutaraldehyde for two hours. The dehydration process was carried out by submerging the samples in low- to high-percentage alcohols within 3 hours, and the samples were dried within 24 hours at ambient temperature (26, 28, 29).

DAPI staining

To count the number of cells proliferated on the scaffold surfaces and compare the results with MTT analysis results, staining was carried out using 4,6-diamidino-2-phenylindole dihydrochloride (DAPI; 1:1000; Invitrogen). The scaffold containing a cell was removed from the incubator on the specified day and was washed twice with PBS. Then, 4% cold formaldehyde was poured on the scaffold and it was kept for 20 minutes at a temperature of 4°C. Afterwards, it was kept at room temperature for 5 minutes and was washed two times with PBS. Next, the DAPI solution was poured for 30 seconds on the scaffold and the scaffold was immediately washed with PBS. The scaffolds were examined using a fluorescent microscope (26, 28).

Statistical analysis

All of the experiments were repeated three times, and the results were reported as mean ± SD (standard deviation). The statistical analysis was carried out using the ANOVA (analysis of variance) and Tukey's test methods with P-Value < 0.05 (21, 22).

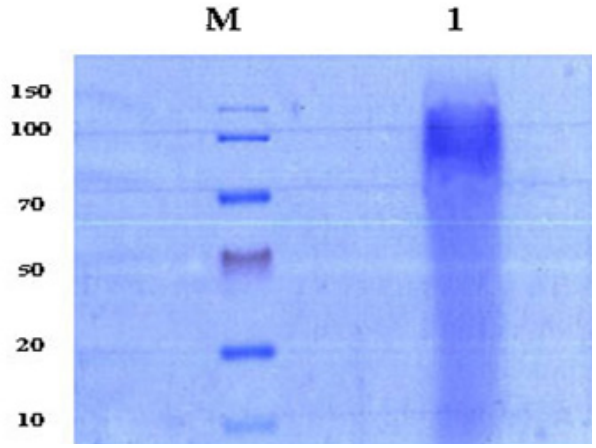

Figure 1. SDS-page analysis of aqueous silk fibroin (ASF). M: Marker; lane 1: ASF.

Results

Molecular mass determination by SDS-Page electrophoresis

As mentioned, the range of the silk fibroin molecular weight resulted from dialysis was determined using the SDS-Page electrophoresis technique. Figure 1 depicts the SDS-Page electrophoresis gel stained with the Coomassie Blue R-250 dye. As seen, the indicator is around the 80 kDa band, which indicates that the molecular weight of the resulting fibroin is in this range.

Functional groups evaluation by ATR-FTIR

Figure 2 shows the levels of fixed and non-fixed silk fibroin samples infrared absorption, which were measured by an ATR-FTIR spectroscopy device.

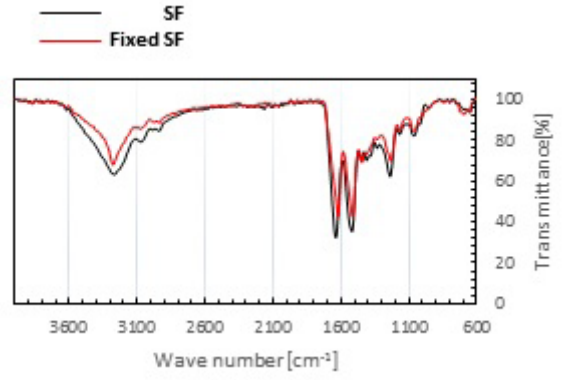

Figure 2. FTIR spectra for the silk fibroin (a) SF, (b) Fixed SF.

Table 1. Viscosity measurement of SF solution in Formic acid at different rpms.

	Viscosity (cp)	Speed (rpm)	% Torque	Shear Rate (1/s)	Temperature (^{0}C)
1	89.50	100.00	17.88	93.00	30.4
2	89.05	105.00	18.67	97.65	30.50
3	88.64	110.00	19.48	102.30	30.58
4	88.26	115.00	20.33	106.95	30.63
5	87.92	120.00	21.10	111.60	30.68
6	88.00	125.00	21.96	116.25	30.70
7	87.69	130.00	22.81	120.90	30.78
8	87.41	135.00	23.62	125.55	30.78
9	87.50	140.00	24.46	130.20	30.78
10	87.24	145.00	25.32	134.85	30.80

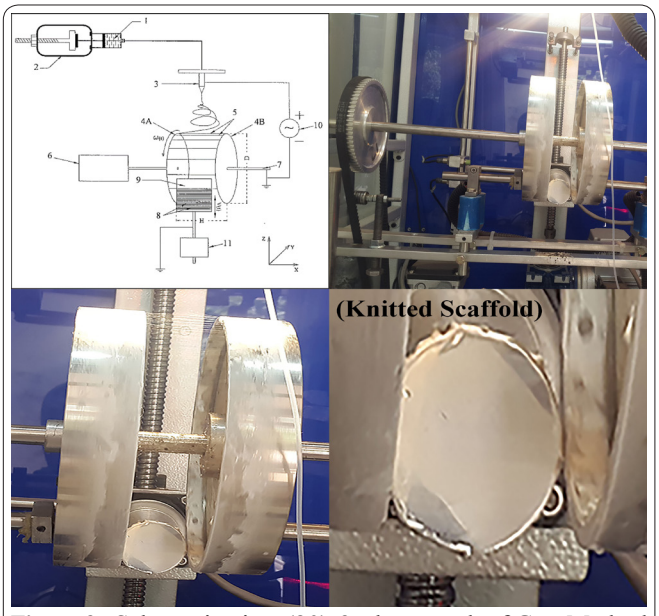

Figure 3. Schematic view (20) & photograph of Gap-Method electrospinning system for knitted scaffold preparation in in three different magnifications.

Viscosity measurement

Table 1 presents the viscosity of the solution obtained from SF (silk fibroin) using the rotational method at different rpms.

Electrospinning procedures

The 20%wt. SF solution in formic acid was electrospun using a GAP-based electrospinning device. Figure 3 shows the schematic view (20) and main view of the electrospinning device in three different magnifications. The nanofibers were prepared with satisfactory precision as knitted and layered fibers with interstitial angles of 60 and 90 degrees.

The numbers in schematic view represents the following: (1) Polymeric solution, (2) Syringe, (3) Electrospinning spinneret, (4A) and (4B) First collector electrodes, (5) Aligned nanofibers, (6) First rotor, (7) Centered maintenance, (8) Knitted scaffold, (9) Second collector, (10) High voltage generator, (11) Second rotor. More information is given in reference 20.

Structural morphology via scanning electron microscopy (SEM)

The following four scaffold samples were prepared and used to study the orientation of the resulting scaffolds, the effect of methanol on the diameter of nanofibers, and the fiber diameter distribution of samples: a) a random scaffold; b) a non-fixed knitted scaffold with a 60-degree angle; c) a methanol-fixed knitted scaffold with a 60-degree angle; and d) a non-fixed knitted scaffold with a 90-degree angle analyzed with SEM. As seen in Figure 4, the nanofiber obtained from the 20%wt. SF solution in formic acid gives soft fibers without any beads. Images of each sample were obtained at four magnification levels.

Mechanical properties

Table 2 shows the tensile properties of the knitted scaffolds with the 60 and 90 weaving angles as compared to a random scaffold. Figure 5 compares the stress-strain graphs in the fixed and non-fixed states for each

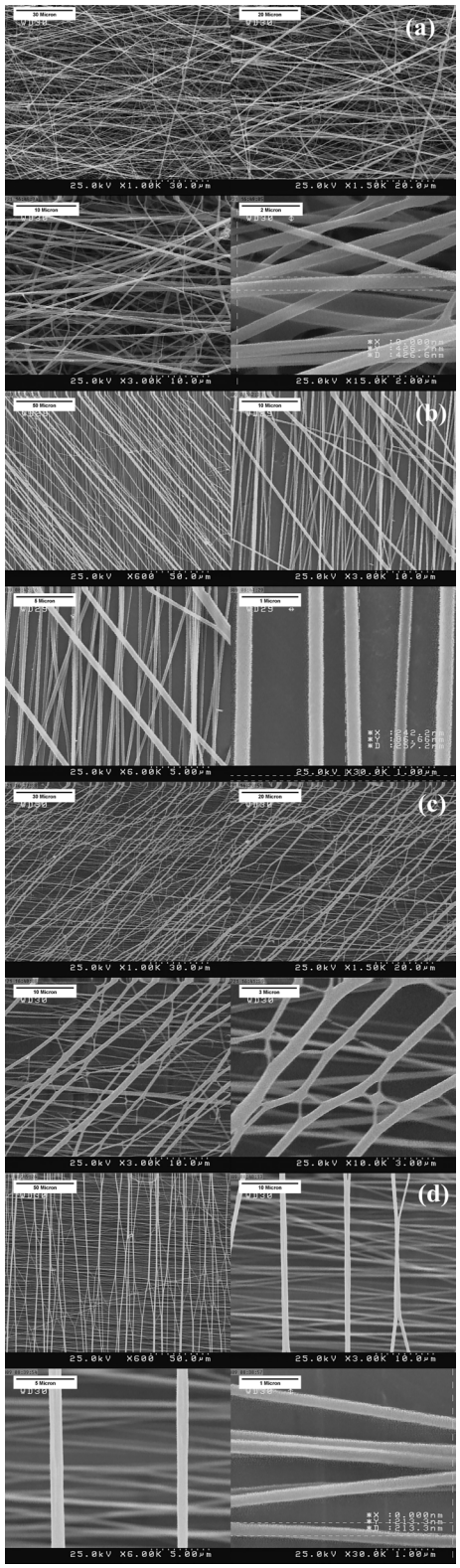

Figure 4. SEM micrograph of electrospun SF fibers (a) Random orientation (b) SF 60 with knitted orientation(Central angle 60˚); (c) SF 60 with knitted orientation(Central angle 600)& Fixed by Methanol immersion (d) SF 90 with knitted orientation(Central angle 90˚).

sample and also compares the three samples in the fixed state.

Porosity measurement

Table 3 shows the porosity of different samples obtained from electrospinning compared to one another before and after cross-linking. As seen in Table 3, all of the samples are in the suitable porosity domain. As compared to the random samples, the knitted samples

Table 1. Viscosity measurement of SF solution in Formic acid at different rpms.

	Module (MPa)	Ultimate Strength (MPa)	Elastic limit Strain (%)
Random	1.40±0.12	1.05±0.07	4.50±0.05
Random-F	2.50±0.14	1.80±0.09	6.00±0.06
SF 60	30.00±2.78	4.40±0.06	7.99±0.10
SF 60-F	150±23.70	15.30±1.03	12.30±0.94
SF 90	1.56±0.80	2.80±0.09	5.90±0.40
SF 90-F	3.10±0.07	4.30±0.20	7.30±1.58

*Random= Electrospun scaffold with random orientation
*Random-F= Electrospun scaffold with random orientation & Fixed by Methanol immersion
*SF 60= Electrospun scaffold with knitted orientation(Central angle 60^0)
*SF 60-F= Electrospun scaffold with knitted orientation(Central angle 60^0) & Fixed by Methanol immersion
*SF 90= Electrospun scaffold with knitted orientation(Central angle 90^0)
*SF 90-F= Electrospun scaffold with knitted orientation(Central angle 90^0) & Fixed by Methanol immersion
Data are expressed as mean (of 5 samples) ± SD
* P<0.05

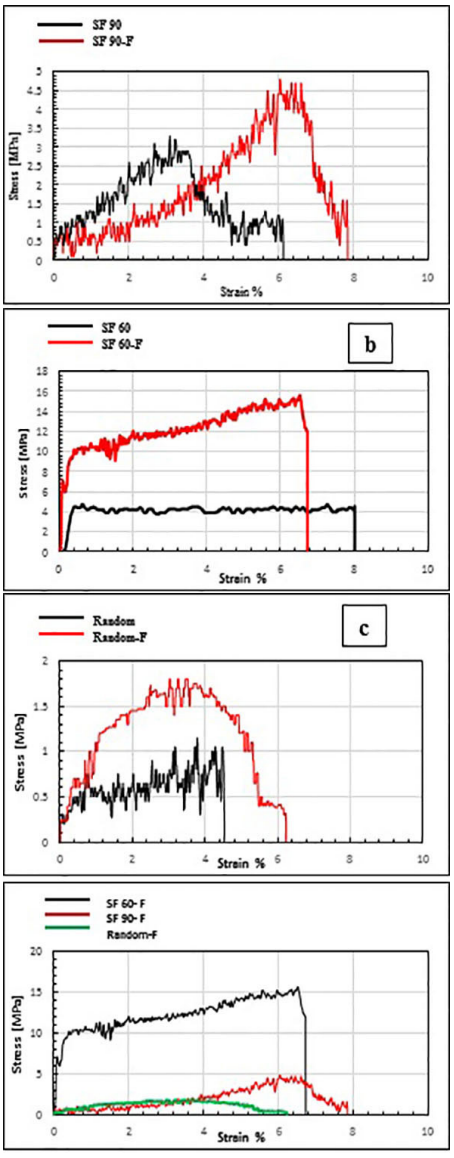

Figure 5. Tensile properties of nanofiber scaffolds (a) Knitted samples with 90˚central angle, (b) Knitted samples with 60˚ central angle, (c) Random samples, (d) comparison of three fixed scaffolds.

Table 3. Porosity measurement of electrospun scaffolds with & without Methanol fixation.

	Porosity %
Random	76.90±3.21
Random-F	73.60±3.40
SF 60	86.20±2.78
SF 60-F	83.90±2.70
SF 90	81.20±2.80
SF 90-F	81.45±2.07

*Random= Electrospun scaffold with random orientation
*Random-F= Electrospun scaffold with random orientation & Fixed by Methanol immersion
*SF 60= Electrospun scaffold with knitted orientation(Central angle 60^0)
*SF 60-F= Electrospun scaffold with knitted orientation(Central angle 60^0) & Fixed by Methanol immersion
*SF 90= Electrospun scaffold with knitted orientation(Central angle 90^0)
*SF 90-F= Electrospun scaffold with knitted orientation(Central angle 90^0) & Fixed by Methanol immersion
Data are expressed as mean (of 5 samples) ± SD
* P<0.05

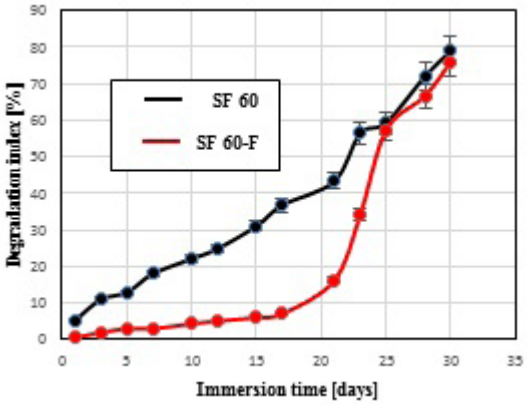

Figure 6. Degradation behavior of SF 60 and SF 60-F samples in different time intervals. N=5, bars represent standard deviation.

demonstrate a higher level of porosity due to the ordered placement of fibers at different levels. The sample with an interstitial angle of 60 degrees shows the highest level of porosity, because arrangement of fibers at this angle provides a smaller inter-surface overlap than the 90-degree arrangement.

Due to a relative increase in the diameter of nanofibers, methanol fixation leads to a less than 2% reduction in the porosity of samples.

Degradation behavior

Of the prepared samples, the SF 60 sample was used for the degradability test. Various physical and chemical mechanisms are involved in the degradation of polymers, and solving and depolymerization are the most common processes.

The results of previous studies suggest that PBS is the optimal choice of degradation solution for in vitro degradation investigation (33, 34). Degradation

solution play a crucial role in the degradation of fibroin. PBS has a stable pH value and osmotic pressure, without oxidation agents or any enzymes, so the degradation of the materials in PBS represents hydrolysis under physiological pH and osmotic pressure. The in vitro degradation of silk fibroin is mainly hydrolysis too. Silk fibroin have different internal structures, namely different contents of α-helices and β-sheets chemical composition. Liu et al. (32) found that a weak base mediated the hydrolysis of the O-peptidyl bond, which leads to silk degradation and the production of a polypeptide mixtures. Previous studies also addressing enzymatic degradation of silk fibroin. Enzymes have little impact on the degradation of silk fibroin but depending on the mode of degradation, silk fibroins can be classified as enzymatically degradable polymers (32, 34).

Contact angle measurement

To reduce the degradation rate of SF scaffolds in water, the pure methanol dehydration method was employed. This chemical operation results in shrinkage and reduced porosity of scaffolds. Moreover, it reduces the number of oxygen-containing groups in the samples. Figure 7 shows the contact angle of a water drop in the first 3 seconds of its collision with the surface of the SF 60-F sample. The cross-linking operation was carried out with methanol on the surface of this sample.

MTT assay

A MTT analysis was conducted to assay the viability and proliferation of fibroblast cells on the surface of SF 60-F (i.e. the knitted methanol-fixed sample with an interstitial angle of 60 degrees, which was exposed to oxygen plasma treatment). Figure 8 presents the ab-

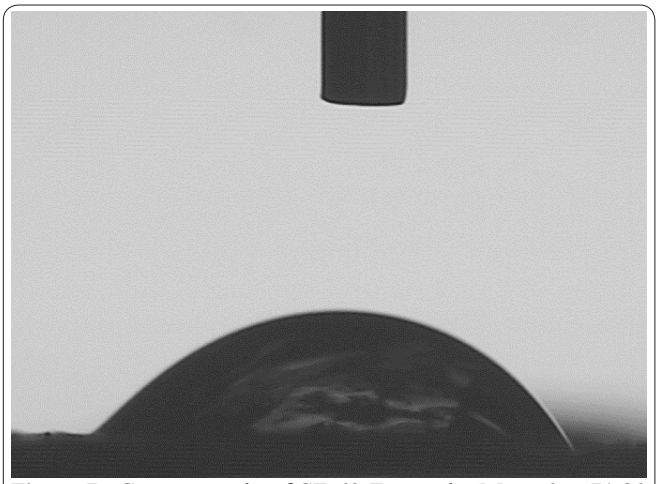

Figure 7. Contact angle of SF 60-F sample. Mean θ = 71.30 ± 0.8(N=5).

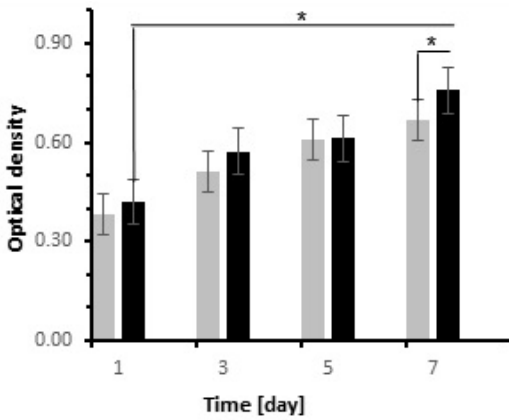

Figure 8. Proliferation of HEK 293 on SF 60-F scaffolds and TCPs during a 7-day culture period (MTT assay): asterisk shows significant difference with $p < 0.05$.

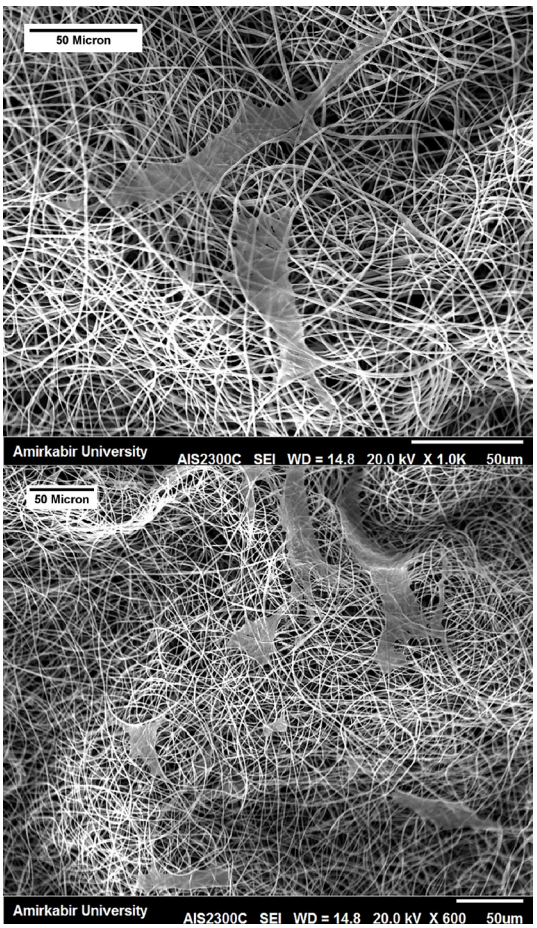

Figure 9. Morphology of HEK 293 on day 3 after seeding at low cell density: SF Random scaffold.

sorption of each sample in the first to seventh days after culture.

Cell morphology analysis

Figure 9 depicts the morphology of cells cultured on the random silk fibroin scaffolds. As seen, after three days of culture, the cells are properly connected and spread over the surface of nanofibers.

DAPI staining

To study the cell counts on the first to seventh days of fibroblasts seeding on the surface of the knitted sample with an interstitial angle of 60 degrees, the DAPI nucleolus staining method was used.

Figure 10 presents the images of samples obtained using a fluorescent microscope with magnification of 10x on the first, third, fifth, and seventh days.

Discussion

The average value of 87.84 cp was used for the production of nanofibers in a suitable cross-section domain. Measurement of viscosity values at various rpms indicated that the 20%wt. fibroin solution in formic acid has an almost invariant viscosity at different shear rates and demonstrates the shear-thinning behavior (Fig. 11).

Fixation through immersion in methanol did not have a significant effect on the morphology of nanofiber surfaces, and as a result of this process only some of the nanofibers merged at the intersections. This result affected the final strength of the fixed scaffold and increased its maximum strength. To study the fiber diameter dis-

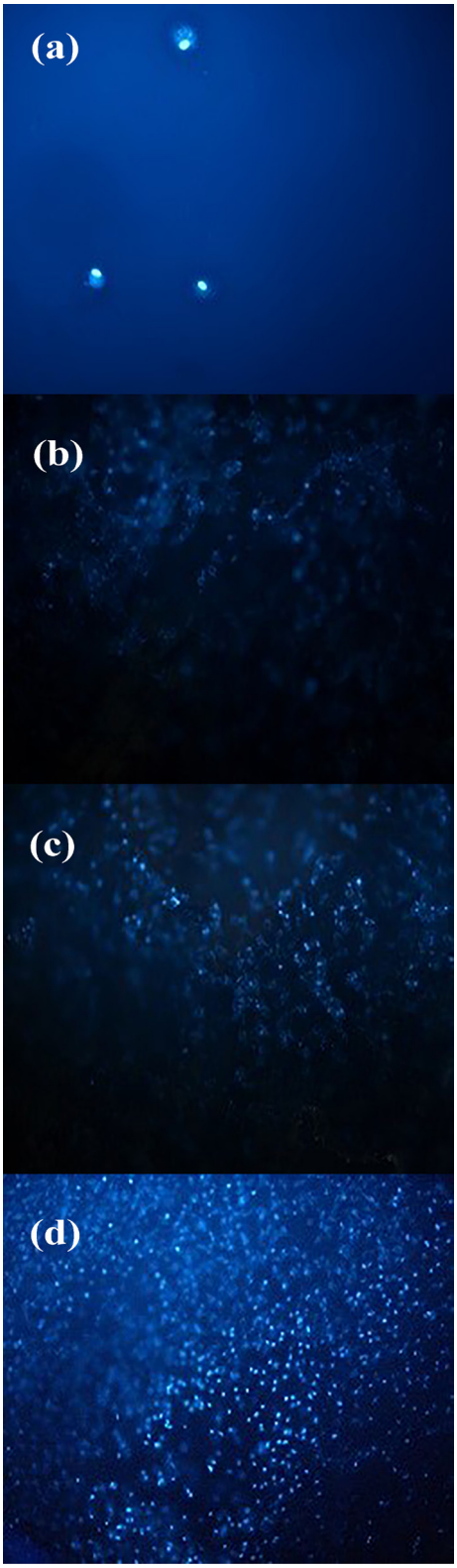

Figure 10. Fluorescence image of HEK 293 grown on SF nanofibrous scaffolds, magnification 10x (a) day 1 after seeding (b) day 3 after seeding (c) day 5 after seeding (d) day 7 after seeding.

tribution of the resulting nanofibers, 100 measurements were carried out on each SEM image. Figure 12 shows the diagonal distribution of samples after the measurements. As seen, the average diameter of fibers in the knitted samples is more uniform while the average diameter of these fibers is lower. In knitted samples, the application of secondary tension in the Gap method, which was the result of the two-phase deposition of fibers, considerably contributed to the uniformity and reduced the diameter of nanofibers. Of the two knitted samples,

Table 4. Infrared absorption picks for different conformations of Silk Amides (18).

	Amide I	Amide II	Amide III
β-Sheet	1625-1648 cm-1	1515-1525 cm-1	1265 cm-1
α-helical	1650- 1658 cm-1	1545 cm-1	1240 cm-1
Random Coil	1640-1648 cm-1	1535-1545 cm-1	1235 cm-1

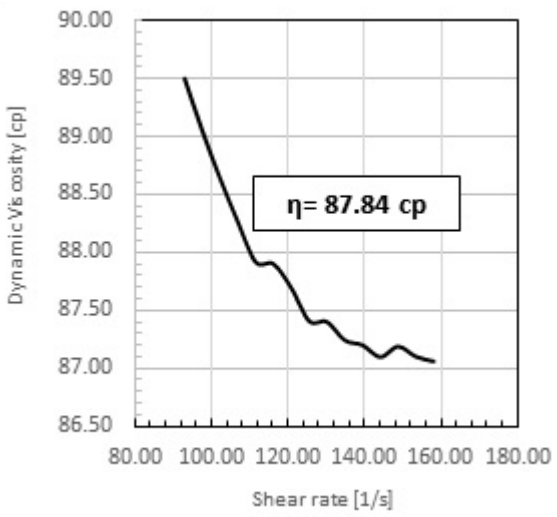

Figure 11. Shear-thinning behavior of SF solution in formic acid (20%wt.).

the sample with an interstitial angle of 60 degrees and average diameter of 230±25nm had the lowest diameter as compared to other samples. Moreover, examination of the effect of methanol revealed that the average diameter of the samples increased to about 280±40nm after cross-linking. This effect was caused by the inflation of fibers following immersion in methanol. This increase along with the merging of fibers led to a reduction in the porosity of the samples.

Mechanical properties show that Silk fibroin (SF) has poor strength properties. As a result, in spite of all of the positive characteristics of SF (such as its biocompatibility and biodegradability), its raw and intact form cannot be used for reconstructive applications, which call for a high level of strength. In previous studies, two methods were often used to increase silk fibroin strength: 1) the post-treatment method; and 2) chemical fixation. In the first method, tension is applied to as-spun fibers to increase strength. This method is not suitable for electrospun scaffolds as it is associated with difficulties. Of the many available chemical fixation methods, fixation through immersion in methanol is the most suitable due to its ease of application and its larger effect on the structure and conformation of molecular chains. The comparisons of the fixed and non-fixed samples suggest that the methanol fixation process increases the maximum strength of samples at the rupture point and also increases their initial modulus. In general, fixation with methanol increases the inter-chain forces and consequently the sample's maximum strength by increasing the β-sheet conformation in the fibroin structure. On the other hand, the β-sheet arrangement does not lead to a significant change in the elongation at break of samples as compared to the non-fixed samples (with a random coil arrangement) due to the increase it causes in the intermolecular order of chains. As a result, methanol fixation normally increases the strength properties of fibroin samples. As seen, the knitted sample with the interstitial angle of 60 degrees has the largest initial modulus and the highest maximum final strength. This is caused by the proper interstitial angle of nanofibers, which along with a proper alignment, proper porosity and optimal density can distribute the force applied to the sample properly between the fibers and prevent early rupture of the sample with the aforementioned initial modulus. Both of the knitted samples demonstrated a higher elongation at break as compared to the random sample. The reason is that a part of the tensile force is applied perpendicular to the interstitial angle of samples, which can reduce the exerted force satisfactorily and prevent failure of the sample. The 60-degree interstitial angle multiplies the final strength by 50 due to the smaller force applied to each angular fiber as compared to the 90-degree angle. However, as seen in Figure 5, the increases in the length of the two knitted samples up to the point of rupture were similar. It could therefore be stated that the knitted tissue highly influences the initial modulus and the maximum strength at break. However, due to a lack of change in the length of molecular chains and the subsequent lack of change in the inter-chain forces under tension, this tissue does not have any considerable effect on the elongation at break.

The nanofiber resulted from electrospinning also has an inter-surface porosity, which results in the three-dimensional structure of the final scaffolds. In medical applications and cell cultures, the satisfactory porosity of scaffolds is about 80%. As compared to the random samples, the knitted samples demonstrate a higher level of porosity due to the ordered placement of fibers at different levels. The sample with an interstitial angle of 60 degrees shows the highest level of porosity, because arrangement of fibers at this angle provides a smaller inter-surface overlap than the 90-degree arrangement. Due to a relative increase in the diameter of nanofibers, methanol fixation leads to a less than 2% reduction in

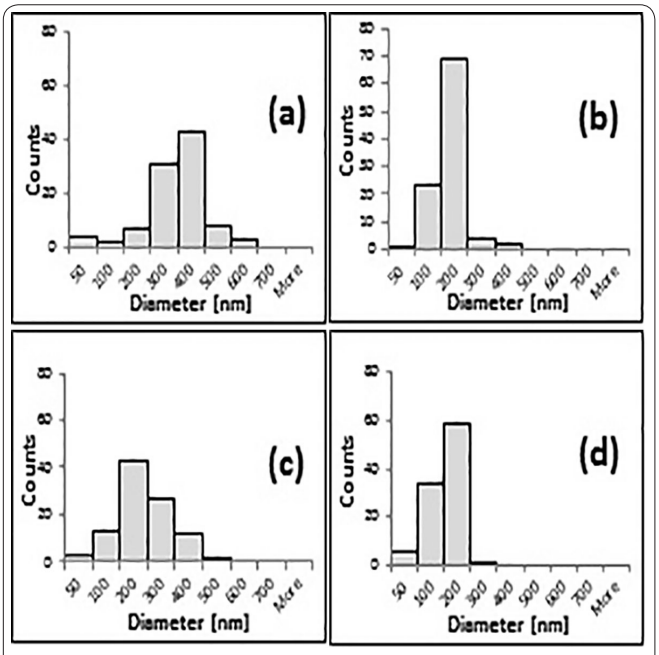

Figure 11. Fiber diameter distribution of (a) Random orientation (b) SF 60 with knitted orientation(Central angle 600); (c) SF 60 with knitted orientation(Central angle 600)& Fixed by Methanol immersion (d) SF 90 with knitted orientation(Central angle 900).

the porosity of samples.

According to degradation results, in the first two weeks, an almost 60% decrease is seen in the weight of the SF 60-F sample, while the SF 60 sample loses 30% of its weight. At the end of the fourth week, both samples lose about 80% of their weights, which indicates that the degradation rate in the SF 60-F sample (fixed with methanol) is similar to that of the non-fixed SF 60 sample in the fourth week. Generally, in view of previous studies, as the content of Silk II with β-sheet conformation increases in the fibroin sample, degradation slows down. This explains the trend of degradation of the methanol-fixed samples in the first two weeks. This is because these samples have more β-sheet content than non-fixed samples. However, the increased degradation rate in the second two weeks can be explained based on the study by Lu et al. for the fixed sample. According to this study, in the fibroin structure, hydrophobic crystal areas with the β-sheet structure are surrounded by the hydrophilic non-crystal zones with the random coil structure. Since the extent of the non-crystal structure is higher in the non-fixed sample, the degradation rate does not grow more rapidly in the first two weeks as compared to the non-fixed sample. At the end of the second week, with the complete omission of the non-crystal areas in the fixed sample, degradation occurs in the crystal areas at a degradation rate similar to the non-fixed sample (35, 33).

After five times contact angle measurement, the average value of θ at different parts of the scaffold was 71.3°± 0.8. The suitable contact angle of scaffolds for medical reconstructive purposes and cell cultures is lower than 60°. Therefore, the sample surface was treated with cold oxygen plasma to increase hydrophilicity. Following the plasma treatment, the samples showed surface water absorption of shorter than 2 seconds and extraordinary hydrophilicity in which obtaining images of the respective contact angle was not possible. All of the samples were exposed to surface plasma treatment prior to the cell culture. Application of oxygen plasma to the sample surface increases surface hydrophilicity by increasing the oxygen-containing functional groups (such as hydroxyl and carboxyl groups) (25, 26).

The absorption of MTT assay shows a growing trend and does not show a considerable reduction as compared to the control samples. This finding reveals the suitable porosity and morphology of the samples. SEM images of cell cultured samples suggests that the application of methanol and plasma to the scaffold surface properly prepared the surface for interaction with cells. Hence, the resulting scaffolds could be easily used as the suitable ECM for cell culture. DAPI staining images indicates that the number of cells on the sample surface increases satisfactorily, which confirms the absorption level resulted from the MTT assay.

In this study, silk fibroin nanofibers were prepared as knitted and angular samples using the Gap electrospinning method. Results indicated that the biocompatibility and biodegradability of the resulting scaffold were similar to the random sample. Therefore, through its tissue structure, this scaffold can be used in tissue engineering and regenerative medicine applications by increasing strength and removing the limited strength of the silk fibroin. Moreover, it can replace previous chemical methods due to its simplicity of production.

Acknowledgments

The study was supported by the Stem cell Research Center, Tehran, Iran.

References

1. Zhang X, Reagan M.R, Kaplan D.L. Electrospun silk biomaterial scaffolds for regenerative medicine. Adv Drug Deliv Rev 2009; 61:988-1006.
2. Fan S, Zhang Y, Shao H, Hu X. Electrospun regenerated silk fibroin mats with enhanced mechanical properties. Int J Biol Macromol 2013; 56:83-88.
3. Sionkowska A, Płanecka A. Preparation and characterization of silk fibroin/chitosan composite sponges for tissue engineering. J Mol Liq 2013; 178:5-14.
4. Jafari M, Paknejad Z, Rezai Rad M, Motamedian SR, Eghbal MJ, Nadjmi N et al. Polymeric scaffolds in tissue engineering: a literature review. J Biomed Mater Res Part B 2015.
5. Kuo C.K, Marturano J.E, Tuan R.S. Novel strategies in tendon and ligament tissue engineering: Advanced biomaterials and regeneration motifs. Sports Med Arthrosc Rehabil Ther Technol 2010; 2:20-27.
6. Wang D, Liu H, Fan Y. Silk Fibroin for Vascular Regeneration. Microsc Res Tech 2015.
7. Hu X, Kaplan D.L. In: Silk Biomaterials. Tufts University, Medford, MA, USA, Elsevier Ltd. 2011, pp. 207-218.
8. Ubaldo A, PraIlaria D, Anna1 Ch, Giuliano F. Will silk fibroin nanofiber scaffolds ever hold a useful place in Translational Regenerative Medicine?. Int J Burn Trauma 2011; 1(1):27-33.
9. Wanga Y, Kima H.J, Vunjak-Novakovicb G, Kaplan D.L. Stem cell-based tissue engineering with silk biomaterials. Biomaterials 2006; 27:6064–6082.
10. Kundu B, Rajkhowa R, Kundu S.C, Wang X. Silk fibroin biomaterials for tissue regenerations. Adv Drug Deliv Rev, September 2012; 65(4):457-70.
11. Arora A, Kothari A, Katti D.S. Pore orientation mediated control of mechanical behavior of scaffolds and its application in cartilage-mimetic scaffold design. J Mech Behav Biomed Mater, 25 June 2015; 51:169-83.
12. Ayutsedea J, Gandhib M, Sukigarac S, Micklusa M, Chend H, Koa F. Regeneration of Bombyx mori silk by electrospinning. Part 3: characterization of electrospun nonwoven mat. Polymer 2005; 46:1625–1634.
13. Kadler K.E, Hill A, Canty-Laird E.G. Collagen fibrillogenesis: fibronectin, integrins, and minor collagens as organizers and nucleators. Curr Opin Cell Biol 2008; 20:495-501.
14. Yang M, Shuai Y, He W, Min S, Zhu L. Preparation of Porous Scaffolds from Silk Fibroin Extracted from the Silk Gland of Bombyx mori (B. mori). Int J Mol Sci 2012; 13:7762-7775.
15. Han F, Liu S, Liu X, Pei Y, Bai S, Zhao H et al. Woven silk fabric-reinforced silk nanofibrous scaffolds for regenerating load-bearing soft tissues. Acta Biomater 2013; 10(2):921-30.
16. Gholipourmalekabadi M, Mozafari M, Bandehpour M, Salehi M, Sameni M, Caicedo H.H et al. Optimization of nanofibrous silk fibroin scaffolds as a delivery system for bone marrow adherent cells. Biotechnol Appl Biochem 2015; 62(6):785–794.
17. Wang H, Zhang Y. Effect of regeneration of liquid silk fibroin on its structure and characterization. Soft Matter, 2012; 9:138-145.
18. Solanas C, Herrero S, Dasari A, Plaza G.R, Lorca J, Perez-Rigueiro J et al. Insights into the production and characterization of electrospun fibers from regenerated silk fibroin. Eur Polym J 2014; 60:123–134.

19. Mallepally R.R, Marin M.A, Surampudi V, Subia B, Rao R.R and Kundu S.C et al. Silk fibroin aerogels: potential scaffolds for tissue engineering applications. Biomed Mater 2015; 10(3):035002.
20. Mohammadi Y, Gazme A, Soleimani M, Haddadi-Asl V. Apparatus and method for electrospinning 2D- or 3D-structures of micro- or nano-fibrous Materials. EP 2045375 A1, 2007.
21. Shafiee A, Soleimani M, Chamheidari GA, Seyedjafari E, Dodel M, Atashi A et al. Electrospun nanofiber-based regeneration of cartilage enhanced by mesenchymal stem cells. J Biomed Mater Res Part A 2011; 99(3):467-78.
22. Naghavi Alhosseini S, Moztarzadeh F, Mozafari M, Asgari Sh, Dodel M, Samadikuchaksaraei A et al. Synthesis and characterization of electrospun polyvinyl alcohol nanofibrous scaffolds modified by blending with chitosan for neural tissue engineering. Int J Nanomedicine 2012; 7:25-34.
23. Hanaee Ahvaz H, Soleimani M, Mobasheri H, Bakhshandeh B, Shakhssalim N, Soudi S et al. Effective combination of hydrostatic pressure and aligned nanofibrous scaffolds on human bladder smooth muscle cells: implication for bladder tissue engineering. J Mater Sci: Mater Med 2012; 23:2281-2290.
24. Abbasi N, Soudi S, Hayati-Roodbari N, Dodel M, Soleimani M. The Effects of Plasma Treated Electrospun Nanofibrous Poly (ε-Caprolactone) Scaffolds with Different Orientations on Mouse Embryonic Stem Cell Proliferation. Cell J. 2014; 16(3): 245-254.
25. Mansourizadeh F, Asadi A, Oryan Sh, Nematollahzadeh A, Dodel M, Asghari-Vostakolaei M. PLLA/HA Nano composite scaffolds for stem cell proliferation and differentiation in tissue engineering. Mol Biol Res Commun 2013; 2(1-2):1-10.
26. Moghani Ghoroghi F, Beygom Hejazian L, Esmaielzade B, Dodel M, Roudbari M, Nobakht M. Evaluation of the Effect of NT-3 and Biodegradable Poly-L-lactic Acid Nanofiber Scaffolds on Differentiation of Rat Hair Follicle Stem Cells into Neural Cells In Vitro. J Mol Neurosci 2013.
27. Jamshidi Adegani1y F, Langroudi L, Ardeshirylajimi A, Dinarvand P, Dodel M, Doostmohammadi A et al. Coating of electrospun poly(lactic-co-glycolic acid) nanofibers with willemite bioceramic: improvement of bone reconstruction in rat model. Cell Biol Int 2014; 38(11):1271-9.
28. Kabiri M, Oraee-Yazdani S, Dodel M, Hanaee-Ahvaz H, Soudi S, Seyedjafari E et al. Cytocompatibility of a conductive nanofibrous carbon nanotube/poly (l-lactic acid) composite scaffold intended for nerve tissue engineering. EXCLI J 2015; 14:851-860.
29. Seyedjafari E, Soleimani M, Ghaemi N, Shabani I. Nanohydroxyapatite-Coated Electrospun Poly(L-lactide) Nanofibers Enhance Osteogenic Differentiation of Stem Cells and Induce Ectopic Bone Formation. Biomacromolecules 2010; 11:3118-3125.
30. Sashina E.S, Bochek A.M, Novoselov N.P, Kirichenko D.A. Structure and Solubility of Natural Silk Fibroin. Zhurnal Prikl Him 2006; 79(6):881-888.
31. Wang X, Chen X, Yoon K, Fang D, Hsiao B.S, Chu B. High Flux Filtration Medium Based on Nanofibrous Substrate with Hydrophilic Nanocomposite Coating. Environ Sci Technol 2005; 39:7684-7691.
32. Liua B, Songa Y, Jina L, Wang Z, Pua D, Lin Sh et al. Silk structure and degradation. Colloids Surf B Biointerfaces 2015; 131:122–128.
33. P. Partlow B, Pasha Tabatabai A , Leisk G , Cebe P, Blair D , Kaplan D.L. Silk Fibroin Degradation Related to Rheological and Mechanical Properties. Macromol. Biosci 2016; 16:666−675.
34. Cao Y, Wang B. Biodegradation of Silk Biomaterials. Int. J. Mol. Sci. 2009; 10:1514-1524.
35. Lua Q, Zhang B, Lia M, Zuoa B, Kaplan D.L, Huanga Y et al. Degradation Mechanism and Control of Silk Fibroin. Biomacromolecules 2011; 12(4):1080-6.